

Recent advances of transition radiation: fundamentals and applications

Ruoxi Chen^{1,2}, Zheng Gong^{1,2}, Jialin Chen^{1,2,3}, Xinyan Zhang^{1,2}, Xingjian Zhu⁴, Hongsheng Chen^{1,2,5,6,*}, and Xiao Lin^{1,2,*}

¹*Interdisciplinary Center for Quantum Information, State Key Laboratory of Extreme Photonics and Instrumentation, ZJU-Hangzhou Global Scientific and Technological Innovation Center, College of Information Science & Electronic Engineering, Zhejiang University, Hangzhou 310027, China.*

²*International Joint Innovation Center, the Electromagnetics Academy at Zhejiang University, Zhejiang University, Haining 314400, China.*

³*Department of Electrical and Computer Engineering, Technion-Israel Institute of Technology, Haifa 32000, Israel.*

⁴*School of Physics, Zhejiang University, Hangzhou 310027, China.*

⁵*Key Laboratory of Advanced Micro/Nano Electronic Devices & Smart Systems of Zhejiang, Jinhua Institute of Zhejiang University, Zhejiang University, Jinhua 321099, China.*

⁶*Shaoxing Institute of Zhejiang University, Zhejiang University, Shaoxing 312000, China.*

**Corresponding authors: xiaolinzju@zju.edu.cn (X. Lin); hansomchen@zju.edu.cn (H. Chen)*

Transition radiation is a fundamental process of light emission and occurs whenever a charged particle moves across an inhomogeneous region. One feature of transition radiation is that it can create light emission at arbitrary frequency under any particle velocity. Therefore, transition radiation is of significant importance to both fundamental science and practical applications. In this paper, we provide a brief historical review of transition radiation and its recent development. Moreover, we pay special attention to four typical applications of transition radiation, namely the detection of high-energy particles, coherent radiation sources, beam diagnosis, and excitation of surface waves. Finally, we give an outlook for the research tendency of transition radiation, especially its flexible manipulation by exploiting artificially-engineered materials and nanostructures, such as gain materials, metamaterials, spatial-temporal materials, meta-boundaries, and layered structures with a periodic or non-periodic stacking.

Free-electron radiation originates from the particle-matter interaction and is a fundamental process of light emission [1-8]. Since free-electron radiation is able to create light emission at arbitrary frequency, it is of paramount importance to numerous applications [9-15], including high-energy particles detector, particle-beam diagnosis, free-electron lasers, high-power microwave/terahertz sources, electron microscopy, biomedical imaging, medical therapy, optical communications, and security.

Due to the exotic particle-matter interactions, the free-electron radiation could occur under different scenarios. Correspondingly, there are various types of free-electron radiation, including Cherenkov radiation [16-19], transition radiation [20-23], Smith-Purcell radiation [24-28], bremsstrahlung radiation [29-34], and synchrotron radiation [35-40], as shown in Fig. 1. Cherenkov radiation is the most famous type of free-electron radiation, and it occurs in a homogeneous matter only when a charged particle moves with a velocity larger than the Cherenkov threshold, namely the phase velocity of light in that matter [41-45]. Different from Cherenkov radiation, the occurrence of transition radiation has no specific requirement on the particle velocity, and it could happen whenever a charged particle moves across an inhomogeneous region [46-50], such as an optical interface. Smith-Purcell radiation emerges when a charged particle moves parallel and close to the surface of an optical diffraction grating [24-28]. Bremsstrahlung radiation, also known as the braking radiation, would appear if the charge particle decelerates or accelerates [29-34]. Synchrotron radiation originates from the circular motion of charged particles [35-40]. Due to the complexity of particle-matter interactions, the free-electron radiation, such as transition radiation, is a subject of extensive researches over the last several decades and is still a hot topic [51-55].

Below, we focus on the discussion of transition radiation. A brief review of the development of transition radiation is provided, including its interesting history and recent advances. To highlight the importance of transition radiation in science and technology, several typical applications of transition radiation are discussed in depth, ranging from high-energy particle detectors [56-65], coherent radiation source [66-71], beam diagnostics [72-76], to excitation of surface plasmon [77-84]. Due to the recent rapid development in material science and nanotechnology, an outlook on how to flexibly control the behavior of transition radiation is given by exploiting exotic artificially-engineered materials and nanostructures [85-90], including gain materials, spatial-temporal materials, meta-boundaries, and layered structures with a random stacking.

Brief development history of transition radiation

We begin with a brief review of the development history of transition radiation, as summarized in Fig. 2. The simplest case of transition radiation was first proposed by Ginzburg and Frank in 1946 [20] by exploring the bombardment of an electron at the interface between vacuum and a metal. The theory of transition radiation was experimentally confirmed in the visible range by Goldsmith and Jelley in 1959 [91], after the analysis of the collected radiation fields, including their polarization, excitation function and absolute yield. In their setup, a Van de Graaff generator was adopted to produce a 5 mega-electron-volt (MeV) beam bunch, which was then injected towards the vacuum-metal interface. Soon after the discovery of transition radiation, the quantum effect of transition radiation was also investigated by Garibian in 1960 [92].

The development of transition radiation is closely related to the interesting history of Ferrell radiation [93], which is featured with a peak near the plasma frequency in the radiation spectrum. In 1958, Ferrell proposed an approximate theory for the radiation of plasma oscillation and claimed that

under suitable circumstances, the plasma oscillations would give off electromagnetic radiation [93]. Since Ferrell radiation could facilitate the plasma-frequency measurement of metals [93], Ferrell radiation was soon experimentally observed in 1960 [94,95]. In 1961, Silin and Fetisov pointed out that Ferrell radiation is merely the transition radiation [96]. In 1962, Stern argued that Ferrell's method and Ginzburg and Frank's theory of transition radiation are two distinct ways to consider the same phenomenon [97]. Stern highlighted that the physical mechanism of Ferrell radiation was misinterpreted by Silin and Fetisov, and it is "a surface effect" [97], namely "the contribution of radiative surface plasma oscillation (SPO)" [98], instead of the bulk longitudinal plasma oscillation in their study. In 1969, Economou emphasized that "there are no radiative SPO in the present geometry" [98]. Actually, he preferred the explanation of transition radiation, after the mathematical analysis of the denominator in the expression of transition radiation near the peak of Ferrell radiation [98]. Due to the recent advances in plasmonics [99-105], it is now acknowledged that the radiative SPO is essentially a leaky mode, denoted as the Ferrell mode [84,97,98,106]. In 2022, the Ferrell radiation was re-investigated in the time domain and was found able to occur far beyond the formation time, since it is supported by a long tail of bulk plasmons following the electron's trajectory deep into the plasmonic medium [107]. This way, the plasmonic tail is capable to mix surface and bulk effects and provides a sustained channel for electron-interface interaction. This time-domain finding may settle the historical debate in Ferrell radiation, regarding whether it is a surface or bulk effect, from transition radiation or plasmonic oscillation. Moreover, with the aid of Ferrell modes in uniaxial epsilon-near-zero materials, such as a thin hexagonal boron nitride (*h*BN) slab, an exotic phenomenon of low-velocity-favored transition radiation was recently proposed [108]. When the low-velocity-favored transition radiation occurs, the light emission from ultralow-energy

particles with extremely-low velocities could exhibit comparable intensity as that from high-energy particles [108].

Due to the recent advances in nanofabrication, artificially-engineered materials or nanostructures, such as metamaterials [109-119], 2D materials [120-128], and photonic crystals [129-135], begin to play an important role in the flexible manipulation of transition radiation.

In 2009, Ref. [136] analyzed the case that a charged particle crosses an interface between a positive-index medium and a negative-index medium. Under this scenario, the transition radiation from the interface and the reversed Cherenkov radiation from the negative-index material would interfere and make the light emission complex. In 2012, Ref. [137] further studied the transition radiation from an average zero-index metamaterial, comprised of periodically alternating negative-index and positive-index layers. A strong radiation enhancement up to three orders of magnitude was predicted, due to the gigantic increase in the density of states at the positive-index/negative-index interface.

In 2012, Ref. [138] used graphene to tailor the transition radiation. Although the graphene is atomically thin, the free electron can efficiently excite graphene plasmons with probabilities in the order of one per electron [139]. In addition to the monolayer graphene [78,84,140-142], Ref. [142] also investigated the photonic and plasmonic transition radiation from multilayer graphene.

Due to the resonance effect, the analysis of transition radiation from periodic structures [143-147] is rather complicated. The related research could be dated back to the transition radiation in a periodically stratified plasma [148]. In 2003, Ref. [149] revealed that the behavior of Cherenkov radiation inside a two-dimensional photonic crystal is intrinsically coupled with the transition radiation and would appear without the Cherenkov threshold. In 2018, Ref. [150] further revealed the

connection between Cherenkov radiation and transition radiation. Actually, Ref. [150] proposed a new mechanism – by exploiting the resonance transition radiation from one-dimensional photonic crystals – to create the effective Cherenkov radiation. This mechanism is capable to control the effective Cherenkov angles with high sensitivity, under any desired range of particle momentum, and is thus promising for the design of novel particle detectors.

High-energy particle detectors based on transition radiation

Particle detectors provide a powerful tool to detect, track and identify high-energy particles [151-155]. In high-energy physics, the charged particle could have a Lorentz factor $\gamma = 1/\sqrt{1 - v^2/c^2}$ up to 10^4 , where v is the particle velocity and c is the speed of light in free space. For such high-energy particles, the sensitivity of common particle detectors (e.g. Cherenkov detectors [156-159]) is generally very low, and thus their detection is full of challenges. To address this issue, Garibian expanded the theory of transition radiation into the X-ray regime in 1959 and found the radiation energy is linearly proportional to the Lorentz factor γ , along with the radiation peak emerging at $\theta_{\max} = \gamma^{-1}$, if $\gamma \gg 1$ [160,161]. Therefore, the unique relation between the radiation energy and the Lorentz factor offers a new route to detect ultra-relativistic particles, even when their kinetic energy is up to tera-eV (TeV). Correspondingly, the particle detector based on the X-ray transition radiation is now known as the transition radiation detector [56-65].

The transition radiation detector, along with other particle detectors, has made a significant contribution to many famous experiments and the finding of new particles (e.g. W and Z bosons [162], the Higgs boson [163]). Actually, the transition radiation detector is widely used in many particle-physics laboratories (e.g. CERN, Femi Lab), as exemplified in Fig. 3. For example, in the H1 experiment, electron and positron were identified at the HERA electron proton collider [56]. In

the experiment E799, the Fermi lab designed a transition radiation detector with a large aperture to provide π/e rejection [57]. In the NOMAD experiment, transition radiation detector discriminated electron and pion and could search for the $\nu_\mu \rightarrow \nu_\tau$ oscillation [58]. In the ALICE experiment, the transition radiation detector is served as a trigger on high $p_t e^+ e^-$ pairs to reduce the collision rate to the readout event rate [59]. In the super proton synchrotron (SPS) of CERN, an inorganic scintillator-based Compton-scatter transition radiation detector in Fig. 3a is designed to detect high-energy electrons with an ultra-high Lorentz factor [60]. In the ATLANS experiment, the transition radiation tracker is a fast detector with thin detector layers realized with straw tubes and could provide both tracking information and particle identification; see its cutaway view in Fig. 3b [61]. In the compressed baryonic matter (CBM) experiment, the transition radiation detector is used to measure common hadrons, such as low-mass dileptons, charmed hadrons, and multistrange baryons [62].

The performance of transition radiation detectors is mainly determined by the properties of the associated radiator and detector. For experiments with relatively-low particle multiplicity, transition radiation detectors generally use multi-wire proportional chambers (MWPC) or straw tubes, filled with a Xenon based gas mixture to efficiently absorb the emitted photons [63]. For experiments with relatively-high particle multiplicity, the efficiency of traditional transition radiation detectors would decrease significantly due to the channel occupancy. Ref. [64] showed that the performance of transition radiation detectors could be improved by replacing MWPC or straw tubes with a high-granularity-micro-pattern gas detector, such as gas electron multipliers as shown in Fig. 3c. In addition, Ref. [150] found that the one-dimensional photonic crystal could create the resonance transition radiation with ultrahigh directivity in Fig. 3d and acts as a new type of radiator.

Correspondingly, the photonic crystal offers a promising versatile platform well suited for the identification of particles at high energy with enhanced sensitivity.

Coherent light sources based on transition radiation

If the electron beam has a length much shorter than the working wavelength, all electrons can be considered to emit in phase. As a result, the related transition radiation is coherent. The phenomenon of coherent transition radiation was first observed in 1991 [164]. One feature of the coherent transition radiation is that its energy could be enhanced by a factor of N than that of the incoherent transition radiation, where N is the electron number.

For any type of free-electron radiation, it takes a finite space domain instead of a point for photons to be emitted. This finite space domain is now known as the formation zone [165], which is a useful concept for the coherent transition radiation. In the context of free-electron radiation, this concept was first presented by Ter-Mikaelian in Landau's seminar in 1952 [166], and later developed by Landau himself [167,168], with its experimental confirmation in the 1990s. Later, Ginzburg extended this concept into transition radiation [169]. The concept of formation zone provides valuable guidance for practical applications based on the transition radiation. Particularly, the influence of formation zone is generally avoided in the design of transition radiation detectors [170].

According to Ginzburg's work [169], the length of the formation zone for the transition radiation, namely the formation length L_f , is defined as the distance that the charge field E^q and the radiation field E^R separate from each other. In other words, the contribution of the interference term $E^q \cdot E^R$ to the total field energy (proportional to $|E^q + E^R|^2$) is very small outside the formation zone. According to the definition, we have

$$L_f = \frac{2\pi}{\left| \omega/v \pm \omega/c \sqrt{1 - \frac{k_\perp^2 c^2}{\omega^2}} \right|} \quad (1)$$

where ω is the angular frequency, k_\perp is the component of wavevector perpendicular to the electron velocity, and \pm correspond to the forward and backward radiation, respectively. Ginzburg's estimation on the formation zone is actually only applicable to the photon emission during the process of transition radiation. In 2017, along the line of Ginzburg's thought, the concept of formation zone was extended to the emitted surface plasmons during the process of transition radiation [78].

With the knowledge of formation zone, the generation of coherent transition radiation mainly relies on two ways. One way is to use an electron beam to directly bombard the optical interface. For example, Ref. [66] shows that the coherent terahertz (THz) radiation could be generated by an electron bunch with a duration in the order of tens of femtoseconds to picoseconds penetrating through the plasma-vacuum interface; see Fig. 4a. Such electron bunches are produced by a laser-plasma accelerator [66]. Similarly, the THz coherent transition radiation with energies in the order of sub-mJ/pulse could also be induced by letting the laser-driven electron beams cross a dielectric-vacuum interface [67] in Fig. 4b. When an electron beam has a femtosecond duration and hundreds of kiloampere peak current and penetrates through the plasma-vacuum interface, the terawatt ultraviolet coherent transition radiation could happen [68]; see the associated ring intensity distribution in Fig. 4c. The other way is to use an ultrahigh-power laser to irradiate on the target material, which further induces the photoelectric effect and makes electrons escape from the rear-side surface of the target material. Ref. [69] shows that the terahertz radiation with a field

strength up to 100 GV/m in Fig. 4d is produced by two-color, ultrashort optical pulses interacting with under-dense helium gases at ultrahigh intensities.

Beam diagnostics based on transition radiation

In order to facilitate the implementation of high-gain free-electron laser or high-power electron beam, the shape of electron beams should be monitored. The coherent transition radiation offers a feasible method to diagnose the electron beam in high-energy equipment. This method mainly relies on the measurement of angular spectral energy density [169]. To be specific, the angular spectral energy density $\frac{d^2W_{\text{total}}}{d\omega d\theta}$ of the coherent transition radiation [169] is

$$\frac{d^2W_{\text{total}}}{d\omega d\theta} \cong N^2 F(\omega) \frac{d^2W_{\text{single}}}{d\omega d\theta} \quad (2)$$

where $\frac{d^2W_{\text{single}}}{d\omega d\theta}$ is the angular spectral energy density for the transition radiation from a single electron, and $F(\omega)$ is a function of longitudinal and transverse distribution parameters for the electron beam after the Fourier transformation. With the knowledge of $\frac{d^2W_{\text{single}}}{d\omega d\theta}$ and $\frac{d^2W_{\text{total}}}{d\omega d\theta}$, the information of electron beams, namely $F(\omega)$, can be straightforwardly obtained in the experiment.

The beam diagnosis based on transition radiation was proposed in 1975 by Ref. [171], which uses two parallel foils. The phase and energy information of electron bunches can be inferred from the angular distribution of the interference pattern of transition radiation. In the following decades, more optical components (e.g. wire grid, Michelson interferometer) are adopted to provide not only the longitudinal and transverse distributions of electron beams but also their divergent angle with the help of coherent transition radiation [72-76].

Figure 5 shows a variety of setups for beam diagnosis, which are widely used in high-energy experiments and facilities, such as free-electron laser, wake-field acceleration, and large particle collider. When the electron beam of 42 MeV passes through an aluminum foil, the coherent transition

radiation with a millimeter or submillimeter wavelength is observed in Fig. 5a [72]. The length of electron beams is measured by using a 45°-tilted foil and a polarizing Michelson interferometer in Fig. 5b, because the spectral power of light emission is dependent on the degree of coherency, which strongly relates to the beam size [73]. More precise measurement for the electron beam is proposed in AWAKE experiments through the usage of seeded self-modulation as shown in Fig. 5c [74]. At the CLARA facility, the coherent transition radiation is used to diagnose the longitudinal beam profile for the dielectric wakefield accelerator and coherent Cherenkov diffraction radiation [75]; see the setup in Fig. 5d.

Excitation of surface wave by using transition radiation

While surface waves can mold the flow of light at the subwavelength scale, their excitation is generally difficult, due to their momentum mismatch with propagating waves. In addition to the conventional schemes like gratings or prism matching, the transition radiation provides a powerful scheme to excite surface waves [77-84], especially for those with extremely-high spatial confinement such as graphene plasmons [78,172-175].

In 1957, Ritchie theoretically proposed a mechanism to excite surface waves by using transition radiation [176]. This prediction was observed in experiments in 2006 [77] by using an electron beam of 50 keV injected onto a flat gold surface as shown in Fig. 6a. In 2017, Ref. [78] theoretically revealed a splashing transient of graphene plasmons launched by swift electrons. During the process of transition radiation, a jet-like rise of excessive charge concentration emerges and is analogous to the hydrodynamic Rayleigh jet in a splashing phenomenon before the launching of ripples. When the free electrons interact with a mesoscopic structure composed of an array of nanoscale holes in a gold film, the surface waves are firstly excited and soon transformed into propagating waves [79]. As a

result, ultrashort chirped electromagnetic wave packets could be created under the irradiation of 30-200 keV electron beams [79]. In 2019, the interaction between free electrons and photonic topological crystals is experimentally studied in Ref. [80]. The robust edge states are excited and observed, when a charged particle passes from one photonic crystal into another one.

Outlook

Despite the numerous applications enabled by the transition radiation, the transition radiation itself still suffers from low intensity and low directionality, especially if the charged particles have ultra-low energy. How to strengthen the particle-interface interaction and control the transition radiation in the desired way remains a long-standing challenge that is highly sought after. While metamaterials, 2D materials, and photonic crystals have been applied to tackle this challenge, there is still plenty of room to tailor the transition radiation by exploiting artificially-engineered materials and nanostructures. For example, we show in Fig. 7 that the gain materials, tilted hyperbolic materials, meta-boundaries, spatial-temporal materials, and layered structures with a periodic or random stacking might offer an enticing platform to enhance the particle-interface interaction and to achieve exotic features of transition radiation.

The gain material in Fig. 7a in practice can be implemented, for example, by using negative-resistance components [177-180] (e.g. microwave tunnel diodes) and optically pumped dye molecules [181,182] (e.g. Rhodamine 800 dye molecules). While gain materials could provide a universal way to amplify the light emission, the free-electron radiation from gain systems, including the transition radiation, has been rarely discussed. Particularly, the influence of optical gain and the slab thickness on the directionality of transition radiation remains elusive, while a larger optical gain is generally thought to have a larger enhancement of the intensity of transition radiation. More rich

physics of free-electron radiation could be expected in systems simultaneously with optical gain and optical loss, such as those with parity-time symmetry [183-187]. However, the influence of the interplay between optical gain and optical loss on the transition radiation has never been explored before.

The hyperbolic material [188-196] is a uniaxial material that has a hyperbolic iso-frequency contour and is featured with an extraordinarily-large photonic density state. Due to these unique features, hyperbolic materials can greatly enhance both the particle-matter interaction and the particle-interface interaction. However, once these high- k hyperbolic modes are excited, they cannot be safely coupled into free space, partly due to the existence of total internal reflection and material losses. How to overcome this issue becomes crucial for the development of novel on-chip light sources based on ultralow-energy electrons. To mitigate this issue, the photonic hyper-crystals are experimentally studied in Ref. [197]. The photonic hyper-crystals have combined virtues of strong light outcoupling in photonic crystals and large photonic density-of-states in hyperbolic metamaterials. Moreover, the broadband enhancement of on-chip photon extraction is achievable by using tilted hyperbolic metamaterials in Fig. 7b [198], since their eigenmodes now become momentum-matched with propagating waves in free space. Due to the exotic features of photonic hyper-crystals [197,199,200] and tilted hyperbolic metamaterials [198], the transition radiation from these exotic materials deserves more in-depth exploration.

The judicious design of electromagnetic boundary could provide a key route to control the free-electron radiation, including the transition radiation. Due to the recent advent of two-dimensional materials (e.g. graphene [201-208], h BN [209-217], twisted photonic structures [218-227]) and metasurfaces [89, 228-235], the boundary is uniquely featured with a surface

conductivity, which can be rather complex but provide an extra degree of freedom to regulate the free-electron radiation. Without loss of generality, the boundary with a non-zero surface conductivity is termed as the meta-boundary in Fig. 7c [236]. According to the electromagnetic boundary conditions, the meta-boundary could be categorized into four types, including isotropic, anisotropic, biisotropic and bianisotropic meta-boundaries [236]. While the transition radiation from the simple isotropic meta-boundary (e.g. graphene) has been extensively studied [78,84,140-142], the transition radiation from more complex meta-boundaries remains largely unexplored and awaits more systematic investigation. Due to the powerfulness of metamaterial and meta-boundaries, the manipulation of free-electron radiation (e.g. transition radiation) at will might be enabled by combining meta-boundaries and metamaterials.

Spatial-temporal materials in Fig. 7d, such as photonic-time crystal and temporal metamaterials, have their optical response dependent both on space and time [237-239]. The emergence of spatial-temporal materials gets rid of fundamental limitations presented in space-engineered media and enable many counterintuitive phenomena, such as magnet-free nonreciprocity [240] and Cherenkov radiation in the vacuum [241,242]. Therefore, the spatial-temporal material in principle can provide a versatile platform to tailor the transition radiation. For example, Ref. [243] showed that a swift electron moving in a photonic-time crystal spontaneously emits radiation. When associated with momentum-gap modes, the process of free-electron radiation is exponentially amplified by the modulation of the refractive index [243]. Actually, the exploration of free-electron radiation from spatial-temporal material is still in its infancy.

Due to the appearance of multiple interfaces in layered structures, the transition radiation from each interface of the layered structure may interfere constructively or destructively. This way,

through the judicious structural design, the layered structure may provide an extra degree of freedom to tailor the particle-interface interaction. For example, if the layered structure has a periodic stacking in Fig. 7e, the constructive interface of transition radiation from each interface can be regarded as the excitation of high- k Bloch modes inside the photonic crystals. As advantageous to the high- k modes in hyperbolic materials, the excited high- k Bloch modes in layered structures with a periodic stacking might be safely coupled into free space, due to the umklapp scattering. Therefore, the particle-interface interaction is promising to efficiently extract the information from ultralow-energy electron, which however remains further studies. Moreover, the dispersion is unavoidable in layered structures with a periodic stacking, either from the material-induced dispersion or the structural-periodicity-induced dispersion. How to reduce or even eliminate the dispersion in layered structures so that the dispersionless resonance transition radiation can be created is still a challenge in science and technology.

If the layered structure has a non-periodic stacking in Fig. 7f, the interference of transition radiation from each interface becomes more random but offers more degrees of freedom to tailor the particle-interface interaction. Due to the disappearance of eigenmodes or Bloch modes in the randomly-stacked layered structures, we can no longer predict the behavior of transition radiation simply from the optical response of the randomly-stacked layered structures. To enable the theoretical prediction, the rigorously analytical solution of transition radiation from the layered structures, although being quite tedious, is mandatory. As a result, whether we can achieve the constructive interference of transition radiation from each interface at a specific radiation angle remains elusive. From the perspective of applications, the associated resonance conditions for transition radiation from the randomly-stacked layered structures are highly wanted. Moreover, due

to the non-period nature of the randomly-stacked layered structures, whether they can be adopted to achieve broadband dispersionless resonance transition radiation is also worth further investigation.

Competing interests

The authors declare no competing interests.

Acknowledgement

X.L. acknowledges the support partly from the National Natural Science Fund for Excellent Young Scientists Fund Program (Overseas) of China, the National Natural Science Foundation of China (NSFC) under Grant No. 62175212, Zhejiang Provincial Natural Science Fund Key Project under Grant No. LZ23F050003, the Fundamental Research Funds for the Central Universities (2021FZZX001-19), and Zhejiang University Global Partnership Fund. H.C. acknowledges the support from the Key Research and Development Program of the Ministry of Science and Technology under Grants No. 2022YFA1404704, 2022YFA1404902, and 2022YFA1405200, the National Natural Science Foundation of China (NNSFC) under Grants No.11961141010 and No. 61975176. J.C. acknowledges the support from the Chinese Scholarship Council (CSC No. 202206320287).

Reference

- [1] A. Konečná, F. Iyikanat, & F. J. G. de Abajo, Entangling free electrons and optical excitations, *Sci. Adv.* 8 (2022) eabo7853.
- [2] A. Fisher, et al., Single-pass high-efficiency terahertz free-electron laser, *Nat. Photon.* 16 (2022) 441-447.
- [3] J. S. Hummelt, et al., Coherent Cherenkov-cyclotron radiation excited by an electron beam in a metamaterial waveguide, *Phys. Rev. Lett.* 117 (2016) 237701.
- [5] Y. Yang, et al., Maximal spontaneous photon emission and energy loss from free electrons, *Nat. Phys.* 14 (2018) 894-899.
- [4] L. J. Wong, I. Kaminer, O. Ilic, J. D. Joannopoulos, & M. Soljacic, Towards graphene plasmon-based free-electron infrared to X-ray sources, *Nat. Photon.* 10 (2016) 46-52.
- [6] G. Adamo, et al., Light well: A tunable free-electron light source on a chip, *Phys. Rev. Lett.* 103 (2009) 113901.
- [7] J. Gardelle, J. Labrousse, & J. L. Rullier, Direct observation of beam bunching produced by a high-power microwave free-electron laser, *Phys. Rev. Lett.* 76 (1996) 4532-4535.
- [8] Genevet, P. et al., Controlled steering of Cherenkov surface plasmon wakes with a one-dimensional metamaterial, *Nat. Nanotech.* 10 (2015) 804-809.
- [9] W. Wang, et al., Free-electron lasing at 27 nanometres based on a laser wakefield accelerator, *Nature* 595 (2021) 516-520.
- [10] W. Decking, et al., A MHz-repetition-rate hard X-ray free-electron laser driven by a superconducting linear accelerator, *Nat. Photon.* 14 (2020) 391-397.

- [11] B. McNeil, & N. Thompson, X-ray free-electron lasers, *Nat. Photon.* 4 (2010) 814-821.
- [12] E. Prat, et al., A compact and cost-effective hard X-ray free-electron laser driven by a high-brightness and low-energy electron beam, *Nat. Photon.* 14 (2020) 748-754.
- [13] X. Lin, et al., A Brewster route to Cherenkov detectors, *Nat. Commun.* 12 (2021) 5554.
- [14] I. Nozawa, et al., Measurement of <20 fs bunch length using coherent transition radiation, *Phys. Rev. ST Accel. Beams* 17 (2014) 072803.
- [15] T. Shaffer, E. Pratt, & J. Grimm, Utilizing the power of Cerenkov light with nanotechnology, *Nat. Nanotech.* 12 (2017) 106-117.
- [16] P. A. Cherenkov, Visible glow under exposure of gamma radiation, *Dokl. Akad. Nauk SSSR* 2 (1934) 451-454.
- [17] H. Hu, et al., Surface Dyakonov-Cherenkov radiation, *eLight* 2 (2022) 2.
- [18] H. Hu, et al., Broadband enhancement of Cherenkov radiation using dispersionless plasmons, *Adv. Sci.* 9 (2022) 2200538.
- [19] F. Liu, et al., Integrated Cherenkov radiation emitter eliminating the electron velocity threshold, *Nat. Photon.* 11 (2017) 289-292.
- [20] V. L. Ginzburg, et al., Radiation of a uniformly moving electron due to its transition from one medium into another, *Zh. Eksp. Teor. Fiz.* 16 (1946) 15-28.
- [21] V. L. Ginzburg, & V. N. Tsytovich, Several problems of the theory of transition radiation and transition scattering. *Physics Reports* 49 (1979) 1-89.
- [22] H. Lihn, et al, Observation of stimulated transition radiation, *Phys. Rev. Lett.* 76 (1996) 4163.
- [23] Karataev, P. et al., First observation of the point spread function of optical transition radiation, *Phys. Rev. Lett.* 107 (2011) 174801.
- [24] S. J. Smith, & E. M. Purcell, Visible light from localized surface charges moving across a grating, *Phys. Rev.* 92 (1953) 1069.
- [25] L. Jing, et al., Polarization shaping of free-electron radiation by gradient bianisotropic metasurfaces, *Laser & Photon. Rev.* 15 4 (2021) 2000426.
- [26] I. Kaminer, et al., Spectrally and spatially resolved Smith-Purcell radiation in plasmonic crystals with short-range disorder, *Phys. Rev. X* 7 (2017) 011003.
- [27] Z. Wang, K. Yao, M. Chen, H. Chen, & Y. Liu, Manipulating Smith-Purcell emission with Babinet metasurfaces, *Phys. Rev. Lett.* 117 (2016) 157401.
- [28] K. Mizuno, J. Pae, T. Nozokido, et al., Experimental evidence of the inverse Smith-Purcell effect, *Nature* 328 (1987) 45-47.
- [29] Y. S. Tsai, Pair production and bremsstrahlung of charged leptons, *Rev. Mod. Phys.* 46 (1974) 815.
- [30] L. I. Schiff, Energy-angle distribution of thin target bremsstrahlung, *Phys. Rev.* 83 (1951) 252.
- [31] F. A. Berends, R. Kleiss, P. de Causmaecker, R. Gastmans, & T. T. Wu, Single bremsstrahlung processes in gauge theories, *Phys. Rev. B* 103 (1981) 124-128.
- [32] F. V. Bunkin, & M. V. Fedorov, Bremsstrahlung in a strong radiation field, *Sov. Phys. JETP* 22 (1966) 844-847.
- [33] E. Aprile, et al., Search for light dark matter interactions enhanced by the Migdal effect or Bremsstrahlung in XENON1T, *Phys. Rev. Lett.* 123 (2019) 241803.
- [34] M. Vassholz, & T. Salditt, Observation of electron-induced characteristic X-ray and bremsstrahlung radiation from a waveguide cavity, *Sci. Adv.* 7 (2021) eabd5677.
- [35] F. R. Elder, A. M. Gurewitsch, R. V. Langmuir, & H. C. Pollock, Radiation from electrons in a synchrotron, *Phys. Rev.* 71 (1947) 829-830.
- [36] A. A. Sokolov, & Ternov, I. M. Synchrotron radiation, *Akademia Nauk SSSR* (1966).
- [37] Y. Hikosaka, et al., Coherent control in the extreme ultraviolet and attosecond regime by synchrotron radiation, *Nat. Commun.* 10(2019) 4988.

- [38] F. Xie, et al., Vela pulsar wind nebula X-rays are polarized to near the synchrotron limit, *Nature* 612 (2022) 658-660.
- [39] J. Hastings, D. Siddons, U. van Bürc, R. Hollatz, & U. Bergmann, Mössbauer spectroscopy using synchrotron radiation, *Phys. Rev. Lett.* 66 (1991) 770.
- [40] A. Zholents, & M. J. Zolotarev, Femtosecond x-ray pulses of synchrotron radiation, *Phys. Rev. Lett.* 76 (1996) 912.
- [41] P. Cherenkov, Radiation from high-speed particles, *Science*. 131 (1960) 136-142.
- [42] I. M. Frank, & I. Tamm, Coherent visible radiation of fast electrons passing through matter, *Dokl. Akad. Nauk SSSR* 14 (1937) 109-114.
- [43] I. M. Frank, Optics of light sources moving in refractive media, *Science* 131 (1960) 702-712.
- [44] H. Hu, et al., Nonlocality induced Cherenkov threshold, *Laser & Photon. Rev.* 14 (2020) 2000149.
- [45] Liu, S. et al., Surface polariton Cherenkov light radiation source, *Phys. Rev. Lett.* 109 (2012) 153902.
- [46] V. L. Ginzburg, & V. N. Tsytovich, *Transition Radiation and Transition Scattering*, CRC Press, 1990.
- [47] V. L. Ginzburg, Transition radiation and transition scattering, *Physica Scripta* 1982 (1982) 182.
- [48] H. Boersch, C. Radloff, & G. Sauerbrey, Experimental detection of transition radiation, *Phys. Rev. Lett.* 7 (1961) 52.
- [49] P. Karataev, et al., First observation of the point spread function of optical transition radiation, *Phys. Rev. Lett.* 107 (2011) 174801.
- [50] P. B. Glek, & A. M. Zheltikov, Enhanced coherent transition radiation from midinfrared-laser-driven microplasmas, *Sci. Rep.* 12 (2022) 7660.
- [51] I. Kaminer, et al., Quantum Čerenkov radiation: Spectral cutoffs and the role of spin and orbital angular momentum, *Phys. Rev. X* 6 (2016) 011006.
- [52] V. Ginis, J. Danckaert, I. Veretennicoff, & P. Tassin, Controlling Cherenkov radiation with transformation-optical metamaterials, *Phys. Rev. Lett.* 113 (2014) 167402.
- [53] Z. Su, et al., Manipulating Cherenkov radiation and Smith-Purcell radiation by artificial structures, *Adv. Opt. Mater.* 7 (2019) 1801666.
- [54] V. V. Vorobev, & A. V. Tyukhtin, Nondivergent Cherenkov radiation in a wire metamaterial, *Phys. Rev. Lett.* 108 (2012) 184801.
- [55] H. Ren, X. Deng, Y. Zheng, N. An, & X. Chen, Nonlinear Cherenkov radiation in an anomalous dispersive medium, *Phys. Rev. Lett.* 108 (2012) 223901.
- [56] G. A. Beck, et al., e^\pm identification using the drift chambers and transition radiators of the H1 forward track detector, *Nucl. Instrum. Meth. A* 367 (1995) 228-232.
- [57] G. E. Graham, et al., Design and test results of a transition radiation detector for a Fermilab fixed target rare kaon decay experiment, *Nucl. Instrum. Meth. A* 367 (1995) 224-227.
- [58] G. Bassompierre, et al., Performance of the NOMAD transition radiation detector, *Nucl. Instrum. Meth. A* 411 (1998) 63-74.
- [59] T. Mahmoud, The ALICE transition radiation detector, *Nucl. Instrum. Meth. A* 502 (2003) 127-132.
- [60] G. L. Case, et al., Measurements of Compton scattered transition radiation at high Lorentz factors, *Nucl. Instrum. Meth. A* 524 (2004) 257-263.
- [61] A. Andronic, & J. P. Wessels, Transition radiation detectors, *Nucl. Instrum. Meth. A* 666 (2012) 130-147.

- [62] V. Friese, The CBM experiment at GSI/FAIR, *Nuclear Physics A* 774 (2006) 377-386.
- [63] F. Barbosa, et al., A new Transition radiation detector based on GEM technology, *Nucl. Instrum. Meth. A* 942 (2019) 162356.
- [64] E. Barbarito, et al., A large area transition radiation detector to measure the energy of muons in the Gran Sasso underground laboratory, *Nucl. Instrum. Meth. A* 365 (1995) 214-223.
- [65] K. D. de Vries, & S. Prohira, Coherent transition radiation from the geomagnetically induced current in cosmic-ray air showers: Implications for the anomalous events observed by ANITA, *Phys. Rev. Lett.* 123 (2019) 091102.
- [66] W. P. Leemans, et al., Observation of terahertz emission from a laser-plasma accelerated electron bunch crossing a plasma-vacuum boundary, *Phys. Rev. Lett.* 91 (2003) 074802.
- [67] G. Q. Liao, et al., Demonstration of coherent terahertz transition radiation from relativistic laser-solid interactions, *Phys. Rev. Lett.* 116 (2016) 205003.
- [68] X. Xu, et al., Generation of terawatt attosecond pulses from relativistic transition radiation, *Phys. Rev. Lett.* 126 (2021) 094801.
- [69] J. Déchard, A. Debayle, X. Davoine, L. Gremillet, & L. Bergé, Terahertz pulse generation in underdense relativistic plasmas: From photoionization-induced radiation to coherent transition radiation, *Phys. Rev. Lett.* 120 (2018) 144801.
- [70] G. Adamo, et al., Electron-beam-driven collective-mode metamaterial light source, *Phys. Rev. Lett.* 109 (2012) 217401.
- [71] L. Yi, & T. Fülöp, Coherent diffraction radiation of relativistic terahertz pulses from a laser-driven microplasma waveguide, *Phys. Rev. Lett.* 123 (2019) 094801.
- [72] Y. Shibata, et al., Observation of coherent transition radiation at millimeter and submillimeter wavelengths, *Phys. Rev. A* 45 (1992) R8340.
- [73] A. Murokh, et al., Bunch length measurement of picosecond electron beams from a photoinjector using coherent transition radiation, *Nucl. Instrum. Meth. A* 410 (1998) 452-460.
- [74] F. Braunmueller, M. Martyanov, S. Alberti, & P. Muggli, Novel diagnostic for precise measurement of the modulation frequency of seeded self-modulation via coherent transition radiation in AWAKE, *Nucl. Instrum. Meth. A* 909 (2018) 76-79.
- [75] K. Fedorov, et al., Development of longitudinal beam profile monitor based on coherent transition radiation effect for CLARA accelerator, *Journal of Instrumentation* 15(2020) C06008.
- [76] A. H. Lumpkin, et al., First observation of z-dependent electron-beam microbunching using coherent transition radiation, *Phys. Rev. Lett.* 86 (2001) 79.
- [77] M. V. Bashevoy, et al., Generation of traveling surface plasmon waves by free-electron impact, *Nano letters* 6 (2006) 1113-1115.
- [78] X. Lin, et al., Splashing transients of 2D plasmons launched by swift electrons, *Sci. Adv.* 3 (2017), e1601192.
- [79] N. Talebi, S. Meuret, S. Guo, et al., Merging transformation optics with electron-driven photon sources, *Nat. Commun.* 10 (2019) 599.
- [80] Y. Yu, et al., Transition radiation in photonic topological crystals: quasis resonant excitation of robust edge states by a moving charge, *Phys. Rev. Lett.* 123 (2019) 057402.
- [81] A. Yurtsever, M. Couillard, & D. A. Muller, Formation of guided Cherenkov radiation in silicon-based nanocomposites, *Phys. Rev. Lett.* 100 (2008) 217402.
- [82] F. J. G. de Abajo, Optical excitations in electron microscopy, *Rev. Mod. Phys.* 82 (2010) 209.
- [83] C. H. Chen, & J. Silcox, Detection of optical surface guided modes in thin graphite films by

high-energy electron scattering, *Phys. Rev. Lett.* 35 (1975), 389.

[84] J. Chen, H. Chen, & X. Lin, Photonic and plasmonic transition radiation from graphene, *Journal of Optics* 23 (2021) 034001.

[85] Y. Zhong, et al., Toggling near-field directionality via polarization control of surface waves. *Laser & Photon. Rev.* 15 (2021) 2000388.

[86] Y. Jiang, et al., Group-velocity-controlled and gate-tunable directional excitation of polaritons in graphene-boron nitride heterostructures. *Laser & Photon. Rev.* 12 (2018) 1800049.

[87] M. Kadic, G. W. Milton, M. van Hecke, & M. Wegener, 3D metamaterials, *Nat. Rev. Phys.* 1 (2019) 198-210.

[88] A. M. Urbas, et al., Roadmap on optical metamaterials, *Journal of Optics* 18 (2016) 093005.

[89] O. Quevedo Teruel, et al., Roadmap on metasurfaces, *Journal of Optics* 21(2019) 073002.

[90] K. S. Novoselov, L. Colombo, P. R. Gellert, M. G. Schwab, & K. Kim, A roadmap for graphene, *Nature* 490 (2012) 192-200.

[91] P. Goldsmith & J. V. Jelley, Optical transition radiation from protons entering metal surfaces, *Philosophical Magazine*, 4 (1959) 836-844.

[92] G. M. Garibyan, Phenomenological quantum electrodynamics in the case of two media, *Zhur. Eksptl'. i Teoret. Fiz.* 39 (1960).

[93] R. A. Ferrell, Predicted radiation of plasma oscillations in metal films, *Phys. Rev.* 111 (1958) 1214-1222.

[94] W. Steinmann, Experimental verification of radiation of plasma oscillations in thin silver films, *Phys. Rev. Lett.* 5 (1960) 470-472.

[95] R. W. Brown, P. Wessel, & E. P. Trounson, Plasmon reradiation from silver films, *Phys. Rev. Lett.* 5 (1960) 472-473.

[96] V. P. Silin, & E. P. Fetisov, Interpretation of the electromagnetic radiation from electron passage through metal films, *Phys. Rev. Lett.* 7 (1961) 374-377.

[97] E. A. Stern, Transition radiation from metal films, *Phys. Rev. Lett.* 8 (1962) 7-10.

[98] E. N. Economou, Surface plasmons in thin films, *Phys. Rev.* 182 (1969) 539-554.

[99] X. Lin, et al., All-angle negative refraction of highly squeezed plasmon and phonon polaritons in graphene-boron nitride heterostructures, *Proceedings of the National Academy of Sciences USA* 114 (2017) 6717-6721.

[100] X. Zhang, et al., Confined transverse-electric graphene plasmons in negative refractive-index systems, *npj 2D Materials and Applications* 4 (2020) 25.

[101] M. Chen, et al., Configurable phonon polaritons in twisted α -MoO₃, *Nat. Mater.* 19(2020) 1307-1311 (2020).

[102] N. Wu, et al., Tunable high-Q plasmonic metasurface with multiple surface lattice resonances, *Progress in Electromagnetics Research* 172 (2021) 23-32.

[103] L. Liu, & Z. Li, Spoof surface plasmons arising from corrugated metal surface to structural dispersion waveguide, *Progress in Electromagnetics Research* 173 (2022) 93-127.

[104] T. Low, et al., Polaritons in layered two-dimensional materials, *Nat. Mater.* 16 (2017) 182-194.

[105] D. N. Basov, M. M. Fogler, & G. de Abajo, Polaritons in van der Waals materials, *Science* 354 (2016) aag1992.

[106] N. Yamamoto, K. Araya, A. Toda, & H. Sugiyama, Light emission from surfaces, thin films and particles induced by high-energy electron beam, *Surf. Interface Anal.* 31 (2001) 79-86.

[107] F. Tay, et al., Anomalous free-electron radiation beyond the conventional formation time,

arXiv (2022) 2211.14377.

[108] J. Chen, et al., Low-velocity-favored transition radiation, arXiv (2022) 2212.13066.

[109] S. Xu, et al., Broadband surface-wave transformation cloak, *Proceedings of the National Academy of Sciences* 112 (2015) 7635-7638.

[110] Yao, D. et al. Miniaturized photonic and microwave integrated circuits based on surface plasmon polaritons. *Progress in Electromagnetics Research* 175, 105-125 (2022).

[111] Z. Guo, C. Lu, X. Lin, & X. Ni, Optical hyperbolic metamaterials, *Frontiers in Materials* 9 (2022) 1115744.

[112] Z. Chen, et al., Wide-angle giant photonic spin Hall effect, *Phys. Rev. B* 106 (2022) 075409.

[113] X. Lin and B. Zhang, Normal Doppler frequency shift in negative refractive-index systems, *Laser & Photon. Rev.* 13 (2019) 1900081.

[114] W. J. Padilla, & R. D. Averitt, Imaging with metamaterials, *Nat. Rev. Phys.* 4 (2022) 85-100.

[115] C. Wang, et al., Enhancing directivity of terahertz photoconductive antennas using spoof surface plasmon structure, *New Journal of Physics* 24.7 (2022) 073046.

[116] L. Zhang, et al., Acoustic non-Hermitian skin effect from twisted winding topology, *Nat. Commun.* 12.1 (2021) 6297.

[117] H. Chen, et al., Left-handed materials composed of only S-shaped resonators, *Phys. Rev. E* 70 (2004) 057605.

[118] Z. Fan, et al., Homeostatic neuro-metasurfaces for dynamic wireless channel management, *Sci. Adv.* 8 (2022) eabn7905.

[119] H. Huang, et al., Millimeter-wave wideband high efficiency circular airy OAM multibeam with multiplexing OAM modes based on transmission metasurfaces, *Progress in Electromagnetics Research*, 173 (2022), 151-159.

[120] Y. Jiang et al., Directional polaritonic excitation of circular, Huygens and Janus dipoles in graphene-hexagonal boron nitride heterostructures, *Progress in Electromagnetics Research* 170 (2021) 169-176.

[121] S. Dai, et al. Tunable phonon polaritons in atomically thin van der Waals crystals of boron nitride, *Science* 343 (2014) 1125-1129.

[122] A. J. Giles, et al. Ultralow-loss polaritons in isotopically pure boron nitride, *Nat. Mater.* 17 (2018) 134-139.

[123] H. Hu, X. Lin, and Y. Luo, Free-electron radiation engineering via structured environments, *Progress in Electromagnetics Research*, 171 (2021) 75-88.

[124] C. Wang, et al., Superscattering of light in refractive-index near-zero environments, *Progress in Electromagnetics Research* 168 (2020) 15-23.

[125] S. Huang, et al., From anomalous to normal: temperature dependence of the band gap in two-dimensional black phosphorus, *Phys. Rev. Lett.* 125 (2020) 156802.

[126] S. Huang, et al., Layer-dependent pressure effect on the electronic structure of 2D black phosphorus, *Phys. Rev. Lett.* 127 (2021) 186401.

[127] Wang, F., Wang, C., Chaves, A. et al. Prediction of hyperbolic exciton-polaritons in monolayer black phosphorus, *Nat Commun.* 12, 5628 (2021).

[128] X. Lin, et al., Ab initio study of electronic and optical behavior of two-dimensional silicon carbide, *Journal of Materials Chemistry C* 1 (2013) 2131-2135.

[129] J. Cao, et al., Tamm states and gap topological numbers in photonic crystals, *Progress in Electromagnetics Research* 173 (2022) 141-149.

- [130] Y. Akahane, et al., High-Q photonic nanocavity in a two-dimensional photonic crystal, *Nature* 425 (2003) 944-947.
- [131] J. D. Joannopoulos, et al., *Molding the flow of light*, Princeton Univ. Press, Princeton, NJ (2008).
- [132] B. Xie, et al. Higher-order quantum spin Hall effect in a photonic crystal, *Nat. Commun.* 11 (2020) 3768.
- [133] X. D. Chen, et al. Direct observation of corner states in second-order topological photonic crystal slabs, *Phys. Rev. Lett.* 122 (2019) 233902.
- [134] S. S. Sunku, et al. Photonic crystals for nano-light in moiré graphene superlattices, *Science* 362 (2018) 1153-1156.
- [135] K. Chen, et al. Graphene photonic crystal fibre with strong and tunable light-matter interaction. *Nat. Photon.* 13 (2019) 754-759.
- [136] S. N. Galyamin, A. V. Tyukhtin, A. Kanareykin, & P. Schoessow, Reversed Cherenkov-transition radiation by a charge crossing a left-handed medium boundary, *Phys. Rev. Lett.* 103 (2009) 194802.
- [137] A. Yanai, & U. Levy, Radiation of a uniformly moving line charge in a zero-index metamaterial and other periodic media, *Optics Express* 20 (2012) 18515-18524.
- [138] V. M. Sukharev, M. N. Strikhanov, & A. A. Tishchenko, Transition radiation from graphene, *J. Phys.: Conf. Ser.* 357 (2012) 012015.
- [139] G. de Abajo, F. J. Multiple excitation of confined graphene plasmons by single free electrons, *ACS Nano* 7 (2013) 11409-11419.
- [140] K. C. Zhang, et al., Transition radiation from graphene plasmons by a bunch beam in the terahertz regime, *Optics Express* 25 (2017) 20477-20485.
- [141] K. Akbari, S. Segui, Z. L. Mišković, J. L. Gervasoni, & N. R. Arista, Energy losses and transition radiation in graphene traversed by a fast charged particle under oblique incidence, *Phys. Rev. B* 98 (2018) 195410.
- [142] K. Akbari, Z. L. Miskovic, S. Segui, J. L. Gervasoni, & N. R. Arista, Energy losses and transition radiation in multilayer graphene traversed by a fast charged particle, *ACS Photon.* 4 (2017) 1980-1992.
- [143] A. E. Kaplan, C. T. Law, & P. L. Shkolnikov, X-ray narrow-line transition radiation source based on low-energy electron beams traversing a multilayer nanostructure, *Phys. Rev. E* 52 (1995) 6795.
- [144] B. Pardo, & J. M. Andre, Transition radiation from periodic stratified structures, *Phys. Rev. A* 40 (1989) 1918.
- [145] B. Lastdrager, A. Tip, & J. Verhoeven, Theory of Čerenkov and transition radiation from layered structures, *Phys. Rev. E* 61(2000) 5767.
- [146] B. Pardo, & J. M. André, Classical theory of resonant transition radiation in multilayer structures, *Phys. Rev. E* 63 (2000) 016613.
- [147] K. Yamada, T. Hosokawa, & H. Takenaka, Observation of soft x rays of single-mode resonant transition radiation from a multilayer target with a submicrometer period, *Phys. Rev. A* 59 (1999) 3673.
- [148] K. F. Casey, & C. Yeh, Transition radiation in a periodically stratified plasma, *Phys. Rev. A* 2 (1970) 810.
- [149] C. Luo, M. Ibanescu, S. G. Johnson, & J. D. Joannopoulos, Cerenkov radiation in photonic

crystals, *Science* 299 (2003) 368-371.

[150] X. Lin, et al., Controlling Cherenkov angles with resonance transition radiation, *Nat. Phys.* 14 (2018) 816.

[151] W. Galbraith, & J. V. Jelley, Light pulses from the night sky associated with cosmic rays, *Nature* 171, 349-350 (1953).

[152] T. Ypsilantis, & J. Seguinot, Theory of ring imaging Cherenkov counters, *Nucl. Instrum. Meth. A* 343 (1994) 30-51.

[153] E. Nappi, Aerogel and its applications to RICH detectors, *Nuclear Physics B (Proc. Suppl.)* 6 (1998) 270-276.

[154] A. Abashian, et al., The Belle detector, *Nucl. Instrum. Meth. A* 478 (2002) 117-232.

[155] M. Adinolfi, et al., Performance of the LHCb RICH at the LHC, *Eur. Phys. J. C.* 73 (2013), 2431.

[156] O. Chamberlain, E. Segrè, C. Wiegand, & T. Ypsilantis, Observation of antiprotons, *Phys. Rev.* 100 (1955) 947-950.

[157] J. J. Aubert, et al., Experimental observation of a heavy particle J, *Phys. Rev. Lett.* 33 (1974) 1404-1406.

[158] J. E. Augustin et al., Discovery of a narrow resonance in e^+e^- annihilation, *Phys. Rev. Lett.* 33 (1974) 1406.

[159] IceCube Collaboration, Evidence for high-energy extraterrestrial neutrinos at the IceCube detector, *Science* 342 (2013) 1242856.

[160] G. M. Garibyan, Contribution to the theory of transition radiation, *JETP (USSR)* 33 (1957) 1403.

[161] G. M. Garibyan, Transition radiation effects in particle energy losses, *JETP (USSR)* 37 (1959) 527-533.

[162] D. Haidt, The discovery of the weak neutral currents, *CERN Courier*, 44 (2004) 8, 21.

[163] J. Heilprin, Higgs Boson discovery confirmed after physicists review Large Hadron Collider data at CERN, *Huffington Post* 14 (2013) 03-13.

[164] U. Happek, A. J. Sievers, and E. B. Blum, Observation of coherent transition radiation, *Phys. Rev. Lett.* 67 (1991) 2962.

[165] L. C. L. Yuan, C. L. Wang, H. Uto, & S. Prünster, Formation-zone effect in transition radiation due to ultrarelativistic particles, *Phys. Rev. Lett.* 25 (1970) 1513.

[166] M. L. Ter Mikaelian, High energy electromagnetic processes in condensed media, Wiley, 1972.

[167] L. D. Landau, & I. Pomeranchuk, The limits of applicability of the theory of bremsstrahlung by electrons and of the creation of pairs at large energies, *Dokl. Akad. Nauk SSSR* 92 (1953) 535.

[168] L. D. Landau, & I. Pomeranchuk, Electron cascade process at very high-energies, *Dokl. Akad. Nauk Ser. Fiz* 92 (1953) 735-738.

[169] V. L. Ginzburg, & V. N. Tsytovich, Transition scattering, *Sov. Phys. JETP* 38 (1974) 909.

[170] B. Dolgoshein, Transition radiation detectors, *Nucl. Instrum. Methods. Phys. Res. A* 326 (1993) 434-469.

[171] L. Wartski, S. Roland, J. Lasalle, M. Bolore, & G. Filippi, Interference phenomenon in optical transition radiation and its application to particle beam diagnostics and multiple-scattering measurements, *Journal of Applied Physics* 46 (1975) 3644-3653.

[172] X. Zhang et al., High-efficiency threshold-less Cherenkov radiation generation by a graphene

hyperbolic grating in the terahertz band, *Carbon* 183 (2021) 225-231.

[173] S. Gong, et al., Direction controllable inverse transition radiation from the spatial dispersion in a graphene-dielectric stack, *Photon. Res.* 7(2019) 1154-1160.

[174] G. Dobrik, et al., Large-area nanoengineering of graphene corrugations for visible-frequency graphene plasmons, *Nat. Nanotechnol.* 17 (2022) 61-66.

[175] L. Cui, J. Wang, & M. Sun, Graphene plasmon for optoelectronics, *Reviews in Physics* 6 (2021) 100054.

[176] R. H. Ritchie. Plasma losses by fast electrons in thin films, *Phys. Rev.* 106 (1957) 874.

[177] C. Qian, et al., Breaking the fundamental scattering limit with gain metasurfaces, *Nat. Commun.* 13 (2022) 4383.

[178] D. Ye, K. Chang, L. Ran, & H. Xin, Microwave gain medium with negative refractive index, *Nat. Commun.* 5 (2014) 5841.

[179] W. Xu, W. J. Padilla, and S. Sonkusale, Loss compensation in metamaterials through embedding of active transistor based negative differential resistance circuits, *Opt. Express* 20 (2012) 22406-22411.

[180] T. Jiang, K. Chang, L. M. Si, L. Ran, & H. Xin, Active microwave negative-index metamaterial transmission line with gain, *Phys. Rev. Lett.* 107 (2011) 205503.

[181] I. de Leon, & P. Berini, Amplification of long-range surface plasmons by a dipolar gain medium, *Nat. Photon.* 4 (2010) 382-387.

[182] M. Gather, et al., Net optical gain in a plasmonic waveguide embedded in a fluorescent polymer, *Nat. Photon.* 4 (2010) 457-461.

[183] Y. Yang, et al., Radiative Anti-parity-time plasmonics, *Nat. Commun.* 13 (2022) 7678.

[184] X. Lin, et al., Loss induced amplification of graphene plasmons, *Optics Letters* 41 (2016) 681-684.

[185] Ş. K. Özdemir, et al., Parity-time symmetry and exceptional points in photonics, *Nat. Mater.* 18 (2019) 783-798.

[186] Wu, Y. et al. Observation of parity-time symmetry breaking in a single-spin system, *Science* 364 (2019) 878-880.

[187] Cao, W. et al. Fully integrated parity-time-symmetric electronics, *Nat. Nanotech.* 17 (2022) 262-268.

[188] S. Dai, et al. Graphene on hexagonal boron nitride as a tunable hyperbolic metamaterial, *Nat. Nanotech.* 10 (2015) 682-686.

[189] S. Dai, et al. Subdiffractional focusing and guiding of polaritonic rays in a natural hyperbolic material, *Nat. Commun.* 6 (2015) 6963.

[190] C. Qian, et al. Multifrequency superscattering from subwavelength hyperbolic structures, *ACS Photon.* 5 (2018) 1506-1511.

[191] J. Jiang, X. Lin, & B. Zhang, Broadband negative refraction of highly squeezed hyperbolic polaritons in 2D materials, *Research* (2018) 2532819.

[192] N. C. Passler, et al., Hyperbolic shear polaritons in low-symmetry crystals, *Nature* 602 (2022) 595-600.

[193] A. Poddubny, I. Iorsh, P. Belov, & Y. Kivshar, Hyperbolic metamaterials, *Nat. Photon.* 7 (2013) 948-957.

[194] A. Nemilentsau, T. Low, & G. Hanson, Anisotropic 2D materials for tunable hyperbolic plasmonics, *Phys. Rev. Lett.* 116 (2016) 066804.

[195] E. E. Narimanov, & A. V. Kildishev, Naturally hyperbolic, *Nat. Photon.* 9 (2015) 214-216.

- [196] V. M. García Chocano, J. Christensen, & J. Sánchez-Dehesa, Negative refraction and energy funneling by hyperbolic materials: An experimental demonstration in acoustics, *Phys. Rev. Lett.* 112 (2014) 144301.
- [197] T. Galfsky, J. Gaa, E. E. Narimanov, and V. Menon. Photonic hypercrystals for control of light-matter interactions, *Proc. Natl. Acad. Sci.* 114 (2017) 5125-5129.
- [198] L. Shen, et al., Broadband enhancement of on-chip singlephoton extraction via tilted hyperbolic metamaterials, *Appl. Phys. Rev.* 7 (2020) 021403.
- [199] J. Yang, et al., Near-field excited Archimedean-like tiling patterns in phonon-polaritonic crystals, *ACS Nano* 15 (2021) 9134-9142.
- [200] F. J. Alfaro-Mozaz, et al., Hyperspectral nanoimaging of van der Waals polaritonic crystals, *Nano Lett.* 21 (2021) 7109-7115.
- [201] X. Shi, et al., Superlight inverse Doppler effect, *Nat. Phys.* 14 (2018) 1001-1005.
- [202] Li, Y. et al., Nonlinear co-generation of graphene plasmons for optoelectronic logic operations, *Nat. Commun.* 13 (2022) 3138.
- [203] X. Lin, et al., Transverse-electric Brewster effect enabled by nonmagnetic two-dimensional materials, *Phys. Rev. A* 94 (2016) 023836.
- [204] X. Lin, et al., Tailoring the energy distribution and loss of 2D plasmons, *New Journal of Physics* 18 (2016) 105007.
- [205] J. Zhang, et al., The roadmap of graphene: from fundamental research to broad applications, *Adv. Funct. Mater.* 32 (2022) 2270232.
- [206] X. Guo, et al., Polaritons in van der Waals heterostructures, *Adv. Mater.* (2022) 2201856.
- [207] Q. Zhang, et al. Interface nano-optics with van der Waals polaritons, *Nature* 597 (2021) 187-195.
- [208] X. R. Wang, et al., Optically transparent microwave shielding hybrid film composited by metal mesh and graphene, *Progress in Electromagnetics Research* 170 (2021) 187-197.
- [209] A. Gottscholl, et al., Spin defects in hBN as promising temperature, pressure and magnetic field quantum sensors, *Nat. Commun.* 12 (2021) 4480.
- [210] P. Huang, et al., Ultra-long carrier lifetime in neutral graphene-hBN van der Waals heterostructures under mid-infrared illumination, *Nat. Commun.* 11 (2020) 863.
- [211] M. Y. Musa, et al., Confined transverse electric phonon polaritons in hexagonal boron nitrides, *2D Materials* 5 (2018) 015018.
- [212] A. Bylinkin, et al., Real-space observation of vibrational strong coupling between propagating phonon polaritons and organic molecules, *Nat. Photon.* 15 (2021) 197-202.
- [213] A. J. Giles, et al., Imaging of anomalous internal reflections of hyperbolic phonon-polaritons in hexagonal boron nitride, *Nano Letters* 16 (2016) 3858-3865.
- [214] N. Li, et al., Direct observation of highly confined phonon polaritons in suspended monolayer hexagonal boron nitride, *Nat. Mater.* 20 (2021) 43-48.
- [215] S. Dai, et al., Phonon polaritons in monolayers of hexagonal boron nitride, *Adv. Mater.* 31 (2019) 1806603.
- [216] I. H. Lee, et al., Image polaritons in boron nitride for extreme polariton confinement with low losses, *Nat. Commun.* 11 (2020) 3649.
- [217] S. Dai, et al., Tunable phonon polaritons in atomically thin van der Waals crystals of boron nitride. *Science* 343 (2014) 1125-1129.
- [218] X. Lin et al., Electronic structures of multilayer two-dimensional silicon carbide with oriented

misalignment, *Journal of Materials Chemistry C* 3 (2015) 9057-9062.

[219] M. Papaj, & C. Lewandowski, Plasmonic nonreciprocity driven by band hybridization in moiré materials, *Phys. Rev. Lett.* 125 (2020) 066801.

[220] L. Zhang, et al., Van der Waals heterostructure polaritons with moiré-induced nonlinearity, *Nature* 591 (2021) 61-65.

[221] X. Zhang, et al., Emerging chiral optics from chiral interfaces, *Phys. Rev. B* 103 (2021) 195405.

[222] X. Lin, et al., Chiral plasmons with twisted atomic bilayers, *Phys. Rev. Lett.* 125 (2020) 077401.

[223] Sheng, L. et al. Exotic photonic spin Hall effect from a chiral interface, *Laser & Photonics Reviews* 16 (2022) 2200534.

[224] J. Chen, et al., A perspective of twisted photonic structures, *Appl. Phys. Lett.* 119 (2021) 240501.

[225] L. Brey, T. Stauber, T. Slipchenko, & L. Martín Moreno, Plasmonic Dirac cone in twisted bilayer graphene, *Phys. Rev. Lett.* 125 (2020) 256804.

[226] E. Y. Andrei, et al., The marvels of moiré materials, *Nat. Rev. Mat.* 6 (2021) 201-206.

[227] N. C. H. Hesp, et al., Observation of interband collective excitations in twisted bilayer graphene, *Nat. Phys.* 17 (2021) 1162-1168.

[228] C. Qian, et al., Experimental observation of superscattering, *Phys. Rev. Lett.* 122, 063901 (2019).

[229] T. Han, K. Wen, Z. Xie, & X. Yue, An ultra-thin wideband reflection reduction metasurface based on polarization conversion, *Progress in Electromagnetics Research* 173 (2022) 1-8.

[230] A. Arbabi, et al., Planar metasurface retroreflector, *Nat. Photon.* 11 (2017) 415-420.

[231] N. Yu, et al., Light propagation with phase discontinuities: generalized laws of reflection and refraction, *Science* 334 (2011) 333-337.

[232] S. Sun, et al. Gradient-index meta-surfaces as a bridge linking propagating waves and surface waves, *Nat. Mater.* 11 (2012) 426-431.

[222] N. Yu, & F. Capasso, Flat optics with designer metasurfaces, *Nat. Mater.* 13 (2014) 139-150.

[234] C. Qian, et al., Performing optical logic operations by a diffractive neural network, *Light Sci. Appl.* 9 (2020) 59.

[235] Y. Zhong, et al., Optical interface engineering with on-demand magnetic surface conductivities, *Phys. Rev. B* 106 (2022) 035304.

[236] X. Zhang, et al., A perspective on meta-boundaries, *arXiv* (2022) 2211.00903.

[237] X. Li, et al., A memristors-based dendritic neuron for high-efficiency spatial-temporal information processing, *Adv. Mater.* (2022) 2203684.

[238] E. K. W. Tan, et al., Density modulation of embedded nanoparticles via spatial, temporal, and chemical control elements, *Adv. Mater.* 31 (2019) 1901802.

[239] B. Liao, et al., Spatial-temporal imaging of anisotropic photocarrier dynamics in black phosphorus, *Nano Letters* 17 (2017), 3675-3680.

[240] Z. Yu, & S. Fan, Complete optical isolation created by indirect interband photonic transitions, *Nat. Photon.* 3 (2009) 91-94.

[241] D. Oue, K. Ding, & J. B. Pendry, Čerenkov radiation in vacuum from a superluminal grating, *Phys. Rev. Res.* 4 (2022) 013064.

[242] P. A. Huidobro, E. Galiffi, S. Guenneau, R. V. Craster, & J. B. Pendry, Fresnel drag in

space-time-modulated metamaterials, Proceedings of the National Academy of Sciences 116 (2019) 24943-24948.

[243] A. Dikopoltsev, et al., Light emission by free electrons in photonic time-crystals, Proceedings of the National Academy of Sciences 119 (2022) e2119705119.

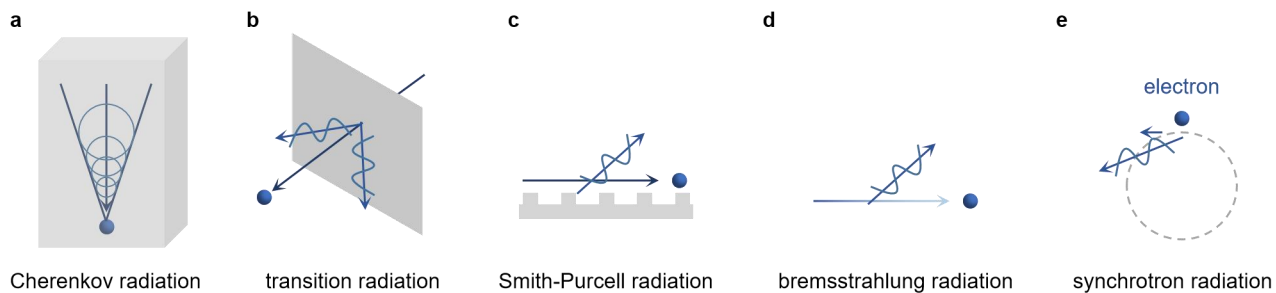


Fig. 1 Schematic of different types of free-electron radiation. a, Cherenkov radiation. **b,** Transition radiation. **c,** Smith-Purcell radiation. **d,** Bremsstrahlung radiation. **e,** Synchrotron radiation.

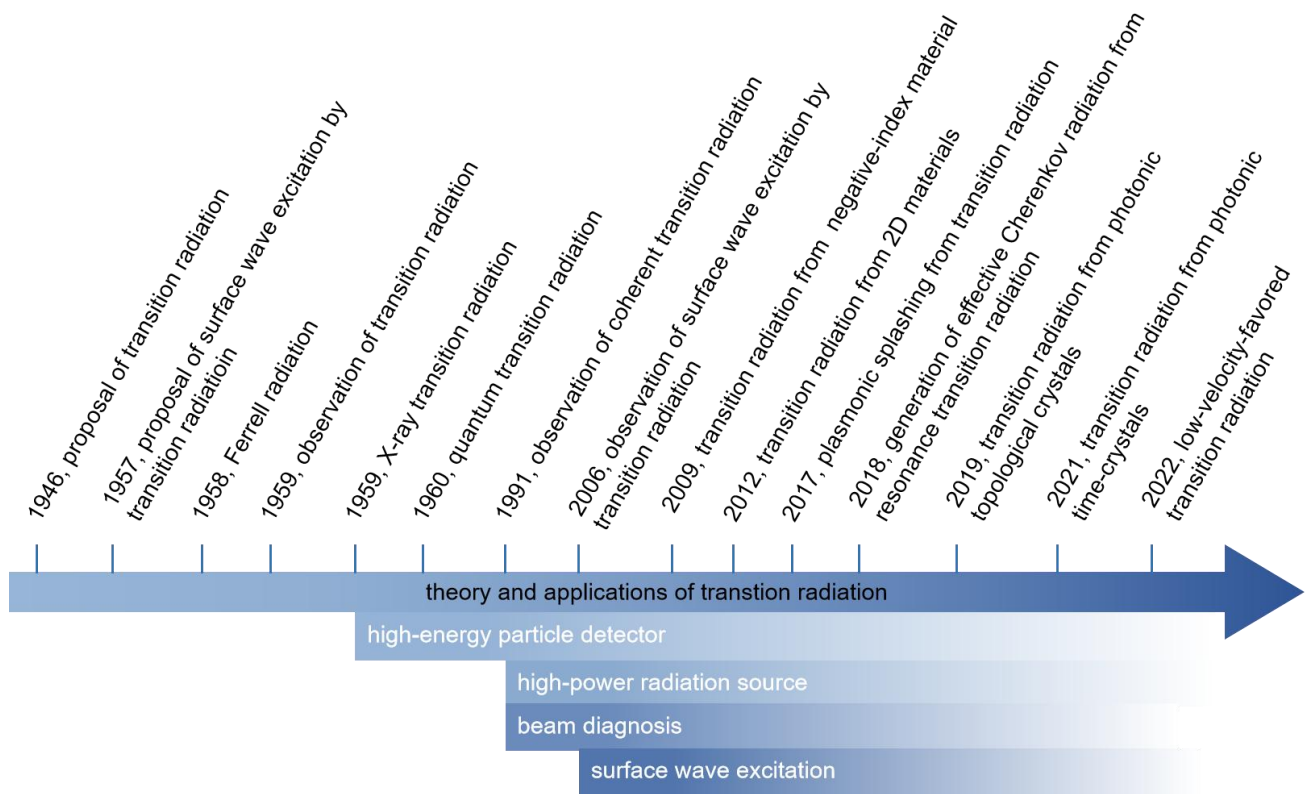


Fig. 2 Brief history of transition radiation, along with its typical applications.

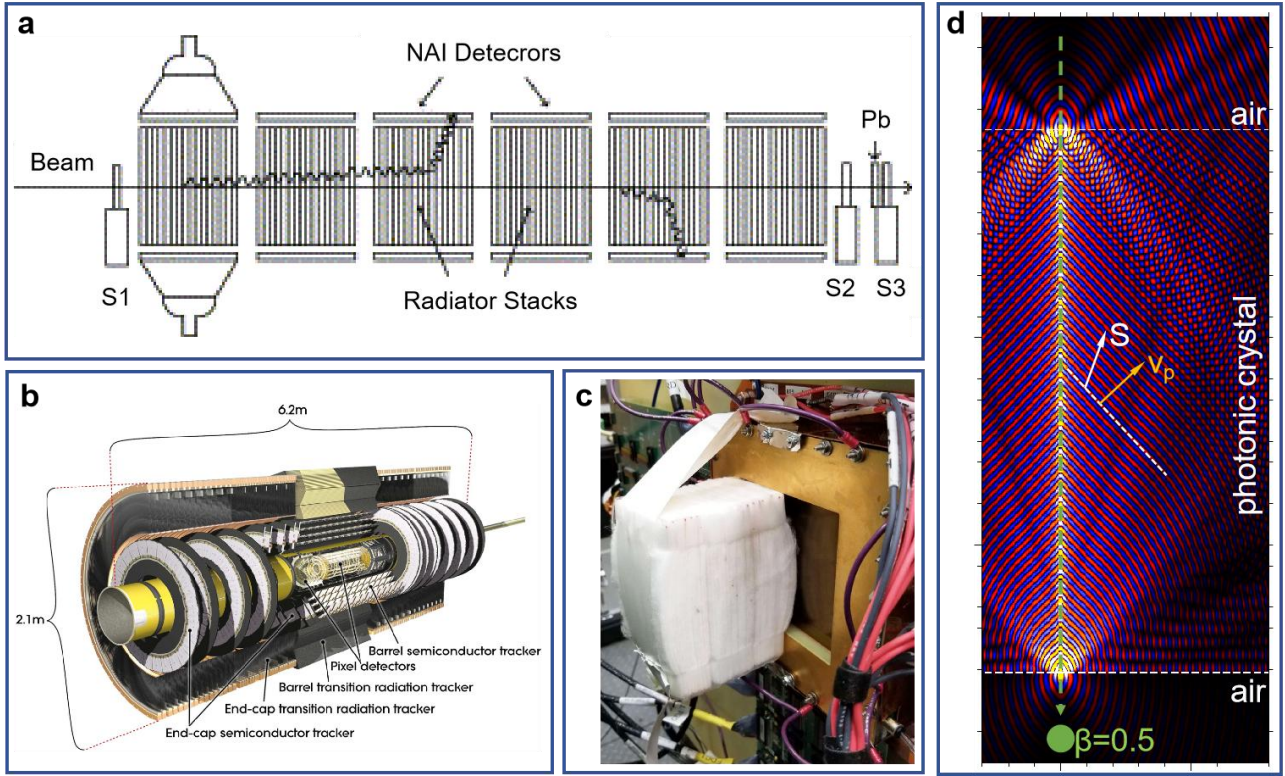


Fig. 3 High-energy particle detectors based on transition radiation. **a**, An inorganic scintillator-based transition radiation detector at the super proton synchrotron (SPS) of CERN [60]. **b**, Cutaway view of the ATLAS inner barrel detectors [61]. **d**, Transition radiation detector based on the gas electron multipliers (GEM) technology [64], which can improve the detector performance to identify multiple particles. **d**, Design of Cherenkov detectors by using the resonance transition radiation [150].

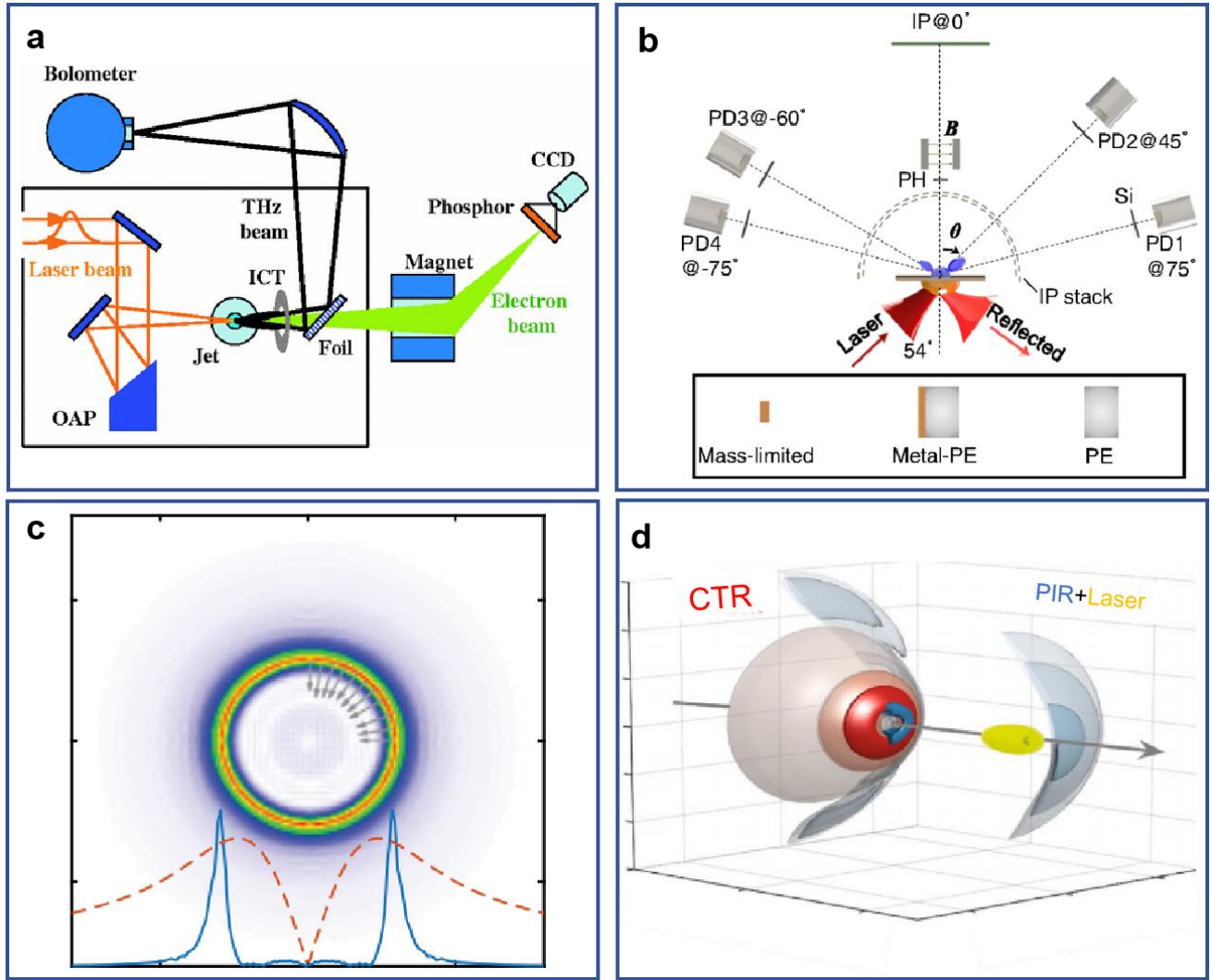


Fig. 4 High-power radiation source by exploiting the coherent transition radiation (CTR). a, High power terahertz emission from a laser-plasma accelerated electron bunch [66]. **b,** Demonstration of terahertz emissions with energy of sub-mJ/pulse [67], when the laser-produced electron beam passes through the rear dielectric-vacuum interface. **c,** Coherent transition radiation by the wakefield-accelerated electrons to yield a field strength of ~ 100 GV/m [68]. **d,** Terawatt attosecond pulses from ultraviolet transition radiation [69].

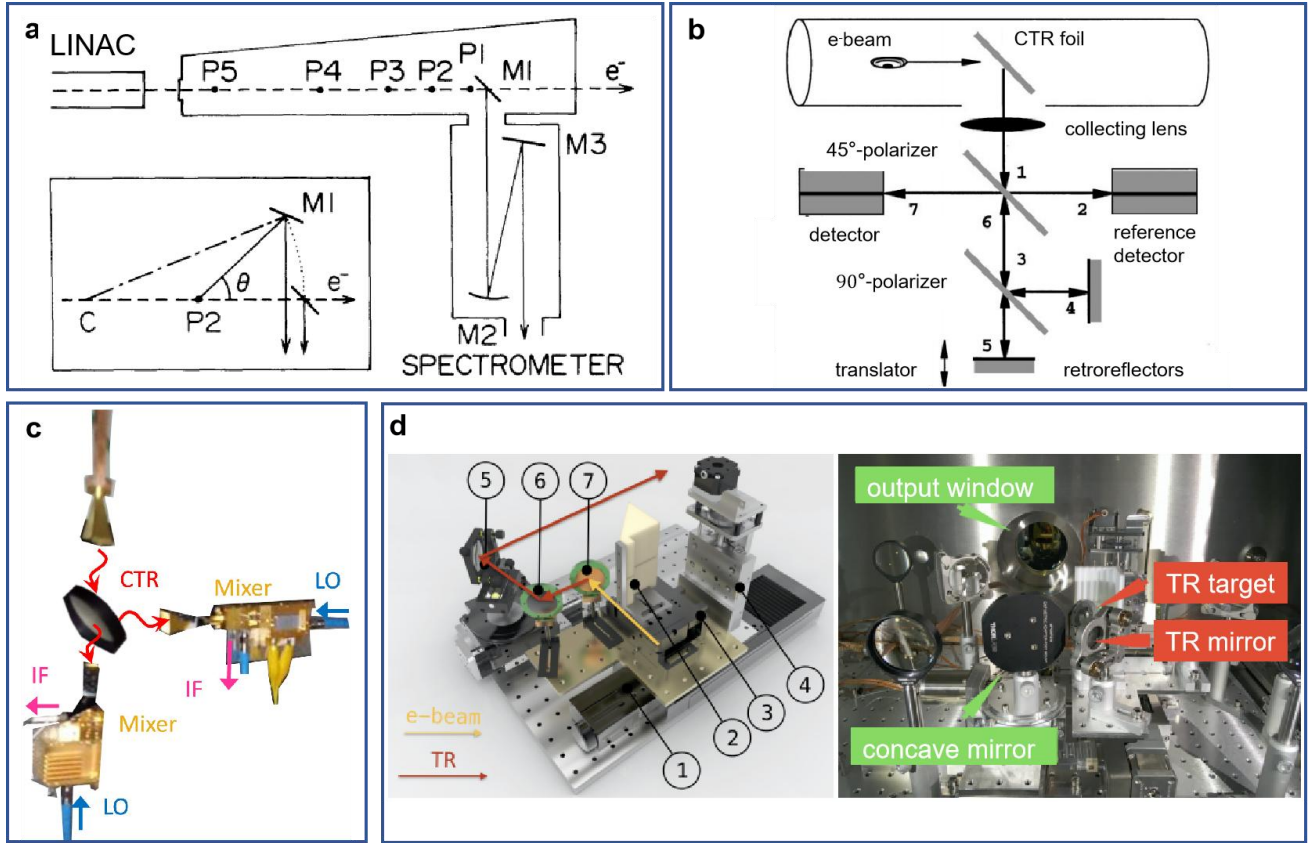


Fig. 5 Beam diagnosis technology based on transition radiation. **a**, Schematic of the experimental setup to observe the coherent transition radiation at millimeter and submillimeter wavelengths [72]. **b**, Bunch length measurement of picosecond electron beams [73]. **c**, A waveguide-integrated heterodyne diagnostic at the AWAKE (Advanced WAKEfield Experiment) of CERN via the coherent transition radiation [74]. **d**, A longitudinal beam profile monitor based on the coherent transition radiation in CLARA (Compact Linear Accelerator for Research and Applications) [75].

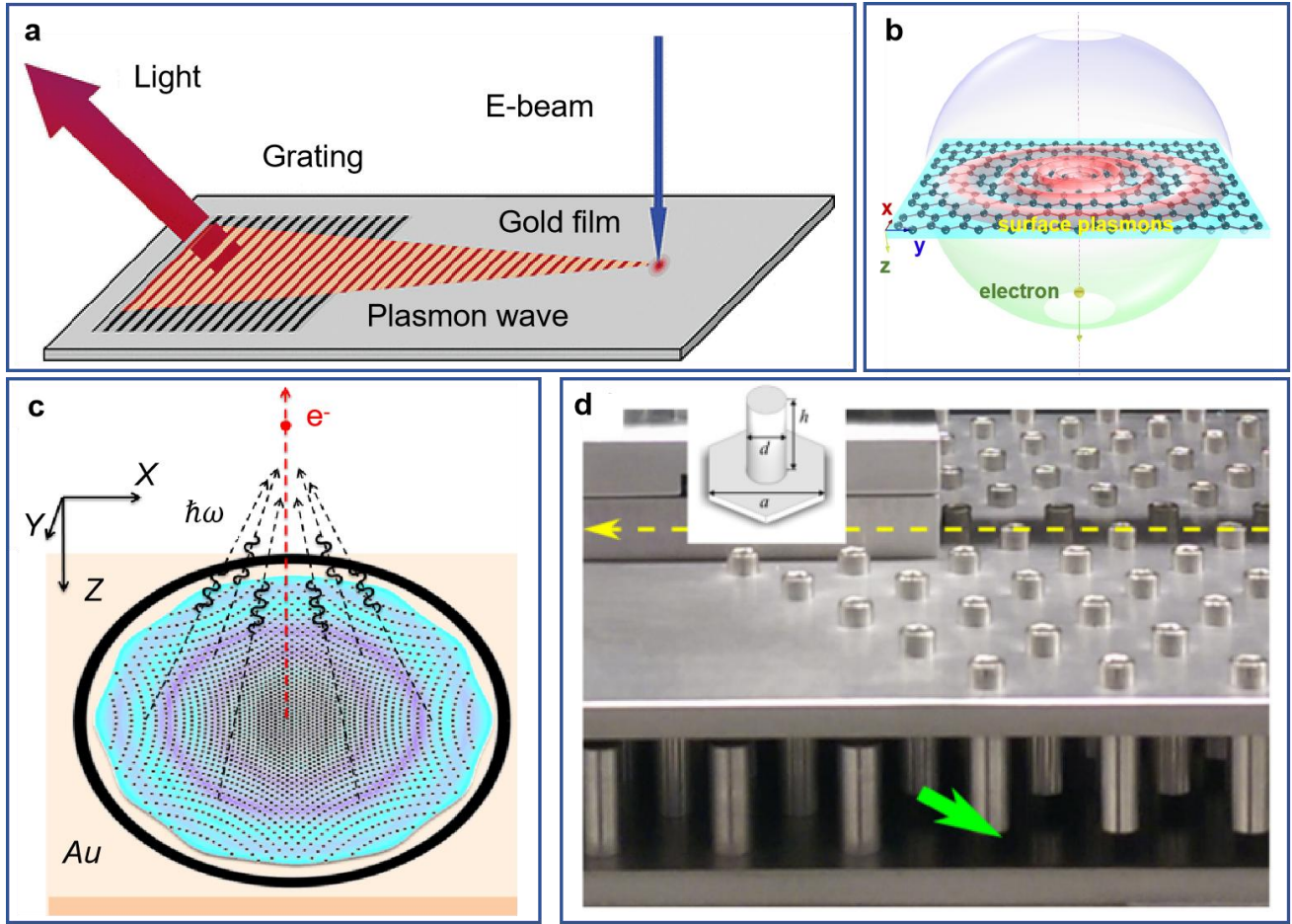


Fig. 6 Excitation of surface waves by transition radiation. **a**, A free-electron beam is injected into a gold surface to create a highly-localized source of surface plasmons [77], which would be further scattered into free space after their interaction with the grating. **b**, Plasmonic splashing from transition radiation [78]. **c**, Femtosecond photon bunches from the coherent scattering of hyperbolic surface waves [79], which are excited by the transition radiation. **d**, Generation of edge waves when an electron beam passes through an interface between two different photonic crystals [80].

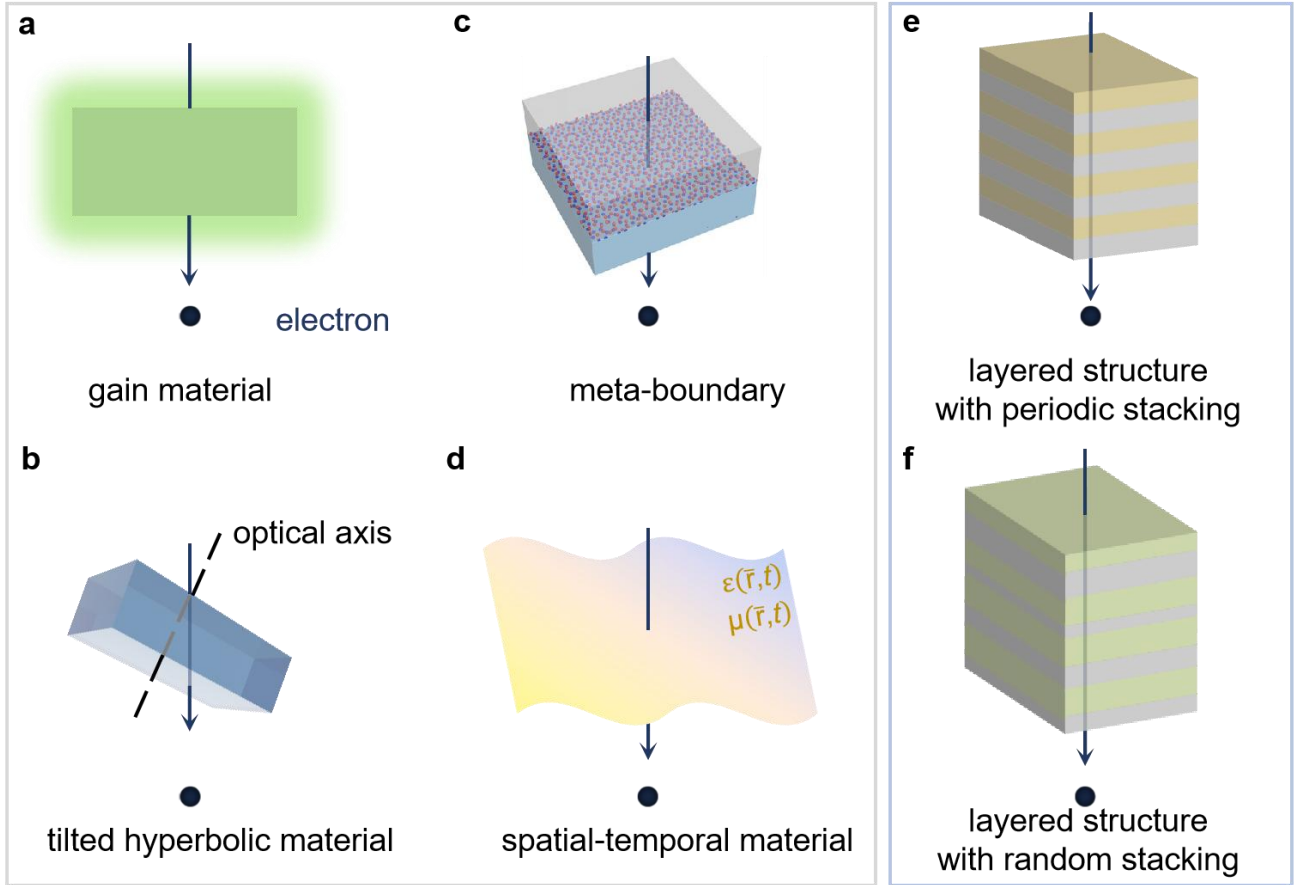


Fig. 7 Manipulation of transition radiation via artificially-engineered materials or nanostructures. **a**, Gain material. **b**, Titled hyperbolic material. **c**, Meta-boundary, such as twisted bilayer graphene. **d**, Spatial-temporal material. **e**, Layered structure with a periodic stacking. **F**, Layered structure with a non-periodic (or random) stacking.